Research Article Vol. 35, No. 11 / November 2018 / Journal of the Optical Society of America A 1899

Journal of the Optical Society of America A

OPTICS, IMAGE SCIENCE, AND VISION

Twisted vortex Gaussian Schell-model beams

C. S. D. Stahl and G. Gbur*

Department of Physics and Optical Science, University of North Carolina at Charlotte, Charlotte, North Carolina 28223, USA
*Corresponding author: gjgbur@uncc.edu

Received 7 September 2018; revised 5 October 2018; accepted 5 October 2018; posted 8 October 2018 (Doc. ID 345383); published 24 October 2018

We introduce a new class of partially coherent vortex beams in which the angular momentum of the beam is provided from two different sources: the underlying vortex of the random beam and the "twist" given to the ensemble of beams. The statistical and propagation properties of such beams are investigated, and their orbital angular momentum properties are analyzed. The combination of distinct orbital angular momentum sources allows unusual behaviors that were previously unobserved.

https://doi.org/10.1364/JOSAA.35.001899

1. INTRODUCTION

In recent years, beams possessing wavefield singularities have become of increasing importance in optical applications. The most familiar singularities are those of scalar waves and they manifest as lines of zero amplitude in 3D space on which the phase of the field is undefined, or singular. Around these lines, the phase has a circulating structure, which had led them to be referred to as *optical vortices*. The study of such vortices, and more sophisticated singularities, has become a subfield of optics in its own right known as *singular optics* [1–3]. Optical vortices have now been employed in a number of applications, including coronagraphy [4], coherence filtering [5], and phase contrast microscopy [6]. Beams with optical vortices also carry orbital angular momentum (OAM), and this angular momentum has been applied to optical tweezing [7] and the design of light-driven machines [8].

Perhaps the most significant application under consideration is the use of vortices in free-space optical communications (FSOC) [9]. It has been shown that information can be multiplexed using different OAM modes, greatly increasing the data transmission rate [10]. However, it has also been demonstrated that atmospheric turbulence tends to induce cross talk between different modes, regardless of whether one uses the topological phase [11] or OAM [12,13] of the beam as the carrier of information.

One strategy for improving the behavior of such beams in turbulence is by making them partially coherent, as partially coherent beams have long been known to have resistance to turbulent fluctuations [14]. Several broad classes of partially coherent beams with OAM are known to exist, including the venerable twisted Gaussian Schell-model (tGSM) beams [15] and a recently discovered class of partially coherent vortex beams we will call Rankine beams [16]. It has been shown that these classes have distinct orbital angular momentum properties [17], with the former acting analogous to a rigid body rotator and the latter acting like a Rankine vortex.

Both the Rankine beams and the tGSM beams [18] can be constructed using a superposition model, in which a weighted ensemble of modes with different transverse axes are incoherently superimposed to produce the cross-spectral density. In the former case, the ensemble is a set of vortex modes, while in the latter case the ensemble is a set of tilted Gaussian modes. The similarity in their design suggests that we can create a beam which combines the features of the two distinct classes of partially coherent OAM beams, which we call twisted *vortex* Gaussian Schell-model beams (tvGSM). Such beams have their OAM determined both by a discrete vortex order as well as a continuous twist parameter, which suggests unprecedented control over the OAM. In this paper we derive the propagation and OAM characteristics of such tvGSM beams.

2. TVGSM MODEL

To study the properties of partially coherent beams, it is most useful to work in the frequency domain with the cross-spectral density function $W(\mathbf{r}_1, \mathbf{r}_2, \omega)$, which can be written as [19]

$$W(\mathbf{r}_1, \mathbf{r}_2, \omega) = \langle \tilde{U}(\mathbf{r}_1, \omega) U(\mathbf{r}_2, \omega) \rangle_\omega, \tag{1}$$

where $\langle \cdots \rangle_\omega$ represents an average over an ensemble of monochromatic fields $U(\mathbf{r}, \omega)$. For convenience, we will use a tilde to represent the complex conjugate throughout the paper. As we will only consider quasi-monochromatic fields, for which the cross-spectral density at a single frequency is a good approximation, we will suppress the expression of ω going forward.

It is to be noted that the cross-spectral density may always be factorized in the following form:

$$W(\mathbf{r}_1, \mathbf{r}_2) = \sqrt{S(\mathbf{r}_1)}\sqrt{S(\mathbf{r}_2)}\mu(\mathbf{r}_1, \mathbf{r}_2), \tag{2}$$

where $S(\mathbf{r})$ is the spectral density, or intensity, of the field at frequency ω, and $\mu(\mathbf{r}_1, \mathbf{r}_2)$ is the spectral degree of coherence. The spectral degree of coherence is a measure of the correlations between the two points, with $|\mu| = 1$ representing full coherence and $|\mu| = 0$ representing complete incoherence.

We consider a cross-spectral density which may be represented as an average over a position-dependent mode $U(\mathbf{r}, \mathbf{r}_0)$, in the form

$$W(\mathbf{r}_1, \mathbf{r}_2) = \int P(\mathbf{r}_0)\tilde{U}(\mathbf{r}_1, \mathbf{r}_0)U(\mathbf{r}_2, \mathbf{r}_0)\mathrm{d}^2 r_0, \tag{3}$$

where the integral is over all transverse positions $\mathbf{r}_0$ and $P(\mathbf{r}_0)$ is a probability density. We take this probability density to be of Gaussian form

$$P(\mathbf{r}_0) = P_0 \exp[-(x_0^2 + y_0^2)/2\sigma^2], \tag{4}$$

where σ is the width of the probability function. A model of the form of Eq. (3) was originally used in [20] to model a vortex beam with a wandering central axis, and has been referred to as the *beam wander model*. It may also be considered a special case of a general method for devising correlation functions introduced by Gori and Santarsiero [21].

For the Rankine beams [16], the modes in question were taken to be simple Laguerre–Gaussian beam modes, of the form

$$U(\mathbf{r}, \mathbf{r}_0) = \frac{U_0}{\Delta^m} \exp[-[(x - x_0)^2 + (y - y_0)^2]/2\Delta^2] \times [(x - x_0) + i(y - y_0)]^m, \tag{5}$$

where Δ is the width of the Gaussian envelope. For tGSM beams [18], the modes are taken to be fundamental Gaussian modes with position-dependent tilts, of the form

$$U(\mathbf{r}, \mathbf{r}_0) = U_0 \exp[-[(x - x_0)^2 + (y - y_0)^2]/2\Delta^2] \times \exp[2\pi i\alpha(x_0 y - y_0 x)], \tag{6}$$

where α is a real-valued "twist parameter."

For the new class of tvGSM beams, we combine the two mode types into one, of the form

$$U(\mathbf{r}, \mathbf{r}_0) = \frac{U_0}{\Delta^m} \exp[-[(x - x_0)^2 + (y - y_0)^2]/2\Delta^2] \times \exp[2\pi i\alpha(x_0 y - y_0 x)][(x - x_0) + i(y - y_0)]^m, \tag{7}$$

which includes both a position-dependent vortex core along with the tilts that result in the twist phase of a tGSM beam.

To study the propagation of such beams, we can simply propagate the individual modes of Eq. (7) and then combine them using Eq. (3) at any propagation distance. The mode at any distance z can be written in the form

$$U(\mathbf{r}, \mathbf{r}_0, z) = \frac{U_0}{\beta} \exp[ik_0 z]\frac{[(x + iy) - (1 + i\gamma)(x_0 + iy_0)]^m}{(\Delta\beta)^m} \times \exp[|\mathbf{r} - \mathbf{r}_0|^2/2\Delta^2\beta]\exp\left[-i\frac{\pi\gamma\alpha}{\beta}|\mathbf{r}_0|^2\right] \times \exp[2\pi i\alpha(yx_0 - xy_0)/\beta], \tag{8}$$

where

$$\gamma \equiv \frac{2\pi\alpha z}{k_0}, \tag{9}$$

$$\beta \equiv 1 - \frac{z}{ik_0\Delta^2}, \tag{10}$$

and k_0 is the free-space wavenumber. A quick derivation of this result is given in Appendix A. It can be readily shown that Eq. (8) reduces to Eq. (7) when $z = 0$.

On substitution of Eq. (8) into Eq. (3), one can, after quite lengthy derivations, find the following result for the cross-spectral density at any distance z:

$$W(\mathbf{r}_1, \mathbf{r}_2, z) = C(z)F(\mathbf{r}_1, \mathbf{r}_2, z)\sum_{k=0}^{m} a_k (D_1 D_2)^{m-k}. \tag{11}$$

This expression uses a lot of defined functions to make it vaguely comprehensible. First, the series coefficient a_k is of the form

$$a_k = \binom{m}{k}^2 \frac{\Gamma(k + 1)}{A^{4m-2k+2}}, \tag{12}$$

where $\binom{m}{k}$ is the binomial coefficient. The function $C(z)$ is of the form

$$C(z) = (1 + \gamma^2)^m \pi \frac{P_0|U_0|^2}{|\beta|^2}\frac{1}{|\Delta\beta|^{2m}}, \tag{13}$$

which takes into account the trivial propagation properties of the beam. The constant A is defined as

$$A^2 = \frac{1}{\Delta^2|\beta|^2} + \frac{4\pi^2\alpha^2 z^2}{k_0^2\Delta^2|\beta|^2} + \frac{1}{2\sigma^2}, \tag{14}$$

and it is a real-valued factor that helps characterize the spreading properties of the beam. The vortex properties of the beam are represented by the factors D_1 and D_2, which may be written as

$$D_1 \equiv \left[\frac{A^2}{1 - i\gamma} - \frac{1}{2\Delta^2\tilde{\beta}} - \frac{\pi\alpha}{\tilde{\beta}}\right](x_1 - iy_1) - \left[\frac{1}{2\Delta^2\beta} - \frac{\pi\alpha}{\beta}\right](x_2 - iy_2), \tag{15}$$

$$D_2 \equiv \left[\frac{A^2}{1 + i\gamma} - \frac{1}{2\Delta^2\beta} - \frac{\pi\alpha}{\beta}\right](x_2 + iy_2) - \left[\frac{1}{2\Delta^2\tilde{\beta}} - \frac{\pi\alpha}{\tilde{\beta}}\right](x_1 + iy_1). \tag{16}$$

It is trivial to verify that the product $D_1 D_2$ satisfies the Hermitian property necessary for cross-spectral densities, i.e., $W^*(\mathbf{r}_1, \mathbf{r}_2) = W(\mathbf{r}_2, \mathbf{r}_1)$.

The final component of Eq. (11) is $F(\mathbf{r}_1, \mathbf{r}_2, z)$, and one can show that it has the form of a twisted Gaussian Schell-model beam:

$$F(\mathbf{r}_1, \mathbf{r}_2, z) = \exp[-N^2 r_1^2]\exp[-\tilde{N}^2 r_2^2]\exp[-M^2|\mathbf{r}_2 - \mathbf{r}_1|^2] \times \exp\left[\frac{2\pi i\alpha}{A^2|\beta|^2\Delta^2}\mathbf{r}_1 \wedge \mathbf{r}_2\right], \tag{17}$$

where

$$N^2 \equiv \frac{\beta}{4\sigma^2\Delta^2 A^2|\beta|^2} - \frac{2\pi^2\alpha^2 z}{A^2|\beta|^2 ik_0\Delta^2}, \tag{18}$$

$$M^2 \equiv \frac{1}{2A^2|\beta|^2}\left[\frac{1}{2\Delta^4} + 2\pi^2\alpha^2\right], \tag{19}$$

and $\mathbf{r}_1 \wedge \mathbf{r}_2$ represents the z-component of the curl of the two transverse vectors. The derivation of Eq. (11), which is the key formula of the paper, is rather lengthy and an outline of it is therefore relegated to Appendix B.

We may broadly separate the noteworthy characteristics of the beam into three categories: the spatial coherence, the topological characteristics, and the orbital angular momentum. We consider each of these in turn. Going forward, we will take the wavelength $\lambda = 1550$ nm and the beam width $\Delta = 2$ cm.

It is to be noted that, even with these constraints, we have three free parameters to tune the characteristics of the beam: the wander parameter σ, the twist phase α, and the vortex order m. If we want all of our modes to be propagating, the twist phase has an absolute upper maximum of

$$\alpha_{\max} = \frac{k_0}{2\pi\sigma}. \tag{20}$$

This is determined by requiring that the maximum tilt of any mode in Eq. (7) have a transverse wavenumber less than the free-space wavenumber. In practice, for the beam to be paraxial, the value of α must be much smaller than $\alpha_{\max}$.

3. COHERENCE CHARACTERISTICS

Though the structure of the beam is quite complicated in general, the overall width of the beam is characterized by the quantity N^2, which provides both the Gaussian envelope of the beam (real part) as well as its wavefront curvature (imaginary part). From Eq. (18), we may write the beam width $\sigma_S(z)$ as

$$\begin{aligned}\sigma_S(z) &= \sqrt{2}\sigma A|\beta|\Delta \\ &= \sqrt{2\sigma^2 + \Delta^2 + \left(\frac{8\pi^2\alpha^2\sigma^2}{k_0^2} + \frac{1}{k_0^2\Delta^2}\right)z^2}.\end{aligned} \tag{21}$$

It can be seen from this expression that the presence of twist α increases the spreading of the beam on propagation, which is not surprising as the twist manifests in our model as a tilt of the constituent Laguerre–Gaussian beams. In the plane $z = 0$, the width is a combination of the inherent width of the beam Δ as well as the wander σ of the beam, as would be expected.

The spectral density $S(\mathbf{r}, z)$ of the beam may be found from Eq. (11), by setting $\mathbf{r}_1 = \mathbf{r}_2 = \mathbf{r}$. This results in the expression

$$S(\mathbf{r}, z) = C(z)\exp[-r^2/\sigma_S^2]\sum_{k=0}^{m} a_k |Q|^{2(m-k)} r^{2(m-k)}, \tag{22}$$

with

$$Q \equiv \frac{1}{|\beta|^2}\left[\frac{A^2|\beta|^2}{1 - i\gamma} - \frac{1}{\Delta^2} - 2\pi i\alpha\frac{z}{k_0\Delta^2}\right] = \frac{1}{1 - i\gamma}\frac{1}{2\sigma^2}. \tag{23}$$

The sum represents an mth-order polynomial in r^2; it is to be noted that all of the coefficients of the sum are positive, however, which indicates that the spectral density will never be zero, except in the fully coherent limit $\sigma \to 0$. This is in agreement with the general observation, first noted in [20], that zeros of intensity are non-generic in partially coherent fields.

Figure 1(a) illustrates the behavior of the intensity in the source plane for several coherence states. It is to be noted that the intensity minimum in the middle becomes less pronounced as the beam wander increases (coherence decreases). Roughly when $\sigma > \Delta$, the null vanishes entirely. Figure 1(b) shows the intensity in the source plane for several vortex orders. It can be seen that the intensity minimum for higher orders is more robust; evidently it takes much more randomization to fully remove the effects of a higher-order vortex. We will see this quantitatively in the next sections.

As can be seen from Eq. (21), adding a twist phase increases the rate at which the beam spreads on propagation. Figure 2 shows the evolution of a beam with (a) $\alpha = 0$ and with (b) $\alpha = 0.001\alpha_{\max}$, with $\alpha_{\max}$ from Eq. (20). It is clear that the twisted beam spreads much more rapidly than the non-twisted beam, which puts a practical limit on the amount of twist a beam can have for long-range applications.

The spatial coherence of the beam, characterized by the function $\mu(\mathbf{r}_1, \mathbf{r}_2, z)$, is also in general of a very complicated form, due to the presence of phase singularities in the correlation function. However, we can define an overall global degree of coherence as $\sigma_\mu \approx 1/M$, where M is defined by Eq. (19). With some effort, one can find

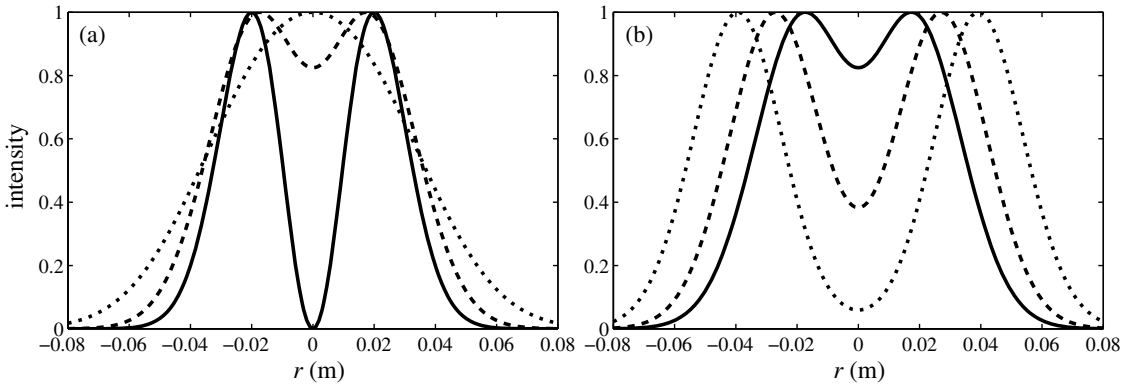

Fig. 1. Intensity of the field in the source plane for (a) different states of coherence and (b) different mode orders. In (a), we have $\sigma = 0.01$ cm (solid), $\sigma = 1$ cm (dashed), and $\sigma = 2$ cm (dotted), with $m = 1$. In (b), we have $m = 1$ (solid), $m = 2$ (dashed), and $m = 4$ (dotted), with $\sigma = 1$ cm.

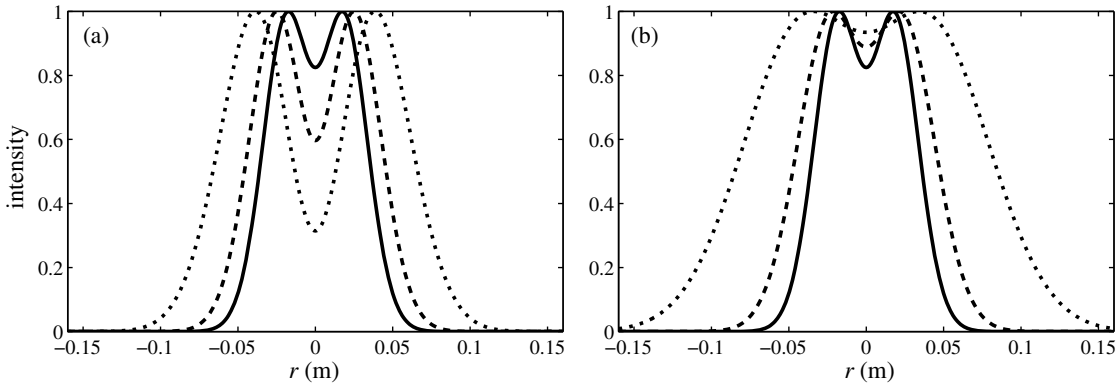

Fig. 2. Intensity of the field on propagation for (a) $\alpha = 0$ and (b) $\alpha = 5 \times 10^{-6}\alpha_{\max}$. The solid lines are $z = 0$, the dashed lines are $z = 2$ km, and the dotted lines are $z = 5$ km. In all cases, $\sigma = 1$ cm and $m = 1$.

$$\sigma_\mu = \sqrt{\frac{\left(\frac{1}{\Delta^2} + \frac{1}{2\sigma^2}\right) + \left(\frac{4\pi^2\alpha^2}{k_0^2\Delta^2} + \frac{1}{k_0^2\Delta^4}\right)z^2}{\frac{1}{4\Delta^4} + \pi^2\alpha^2}}. \tag{24}$$

The presence of the twist term in the numerator indicates that the spatial coherence increases more rapidly with a twist phase present.

It should be noted that the presence of the underlying vortex mode does not contribute at all to the overall spreading of the beam or its correlation function, as m does not appear at all in Eqs. (21) and (24). It does, however, effect the overall transverse profile of the beam, as Eq. (22) indicates, and plays a key role in the topological and OAM properties of the beam, as we will now see.

4. TOPOLOGICAL CHARGE

As tvGSMs are partially coherent fields, the phase of the field is a random function of position and time, and the topological phase properties of the field must be evaluated with some care. Here we consider two approaches to measuring the topology of tvGSMs, each with its advantages and disadvantages.

First, let us imagine that the fluctuations of the field are slow enough that we can instantaneously measure the phase structure of the field, using interferometry or a Shack–Hartmann sensor. Then we may evaluate the measured topological charge for every member of the ensemble, and directly calculate the average topological charge from these results.

Let us assume that we measure the topological charge within an aperture of radius b. Returning to Eq. (8), which represents the member of the ensemble centered on (x_0, y_0), we see that there is an mth-order vortex with topological charge m at a position (x, y), such that

$$(x + iy) = (1 + i\gamma)(x_0 + iy_0), \tag{25}$$

or at a radial position,

$$r = \sqrt{1 + \gamma^2}\, r_0. \tag{26}$$

This vortex will only be measured if $r < b$; otherwise, the measured topological charge is zero. Therefore, the average topological charge of the whole ensemble is of the form

$$\bar{t} = m \int_{r_0 < b/\sqrt{1+\gamma^2}} P(r_0)\mathrm{d}^2 r_0. \tag{27}$$

This integral is readily evaluated, and we find that

$$\bar{t} = m\{1 - \exp[-b^2/2\sigma^2(1 + \gamma^2)]\}. \tag{28}$$

As expected, the average topological charge is equal to m when $\sigma = 0$ (full coherence) and decreases as σ increases. The factor of $1 + \gamma^2$, with γ given by Eq. (9), represents the effect of the twist on the average charge. The more twisted the beam is, the more rapidly the tilted beams will veer outside of the detector radius, causing the charge to be lost.

The aforementioned method is limited not only in the need to measure the phase of the field rapidly, but also in its dependence on the specific ensemble. As is well known, many different ensembles may result in the same cross-spectral density, which means that this average value of topological charge may not be accurate for a particular method of generating a tvGSM.

It is also known, however, that the phase singularities of a coherent field become correlation singularities of the cross-spectral density when the spatial coherence is reduced. We can see this explicitly from Eq. (11), which we write below without all of the constants and envelopes which contribute nothing to the topological structure:

$$\hat{W}(\mathbf{r}_1, \mathbf{r}_2) = \sum_{k=0}^{m} a_k [\tilde{G}\tilde{\eta}_1 - H\tilde{\eta}_2]^{m-k} [G\eta_2 - \tilde{H}\eta_1]^{m-k}, \tag{29}$$

where $\eta_j = x_j + iy_j$, with $j = 1, 2$, and

$$G \equiv \frac{A^2}{1 + i\gamma} - \frac{1}{2\Delta^2\beta} - \frac{\pi\alpha}{\beta}, \tag{30}$$

$$H \equiv \frac{1}{2\Delta^2\beta} - \frac{\pi\alpha}{\beta}. \tag{31}$$

Equation (29) indicates that, generally, $\hat{W}$ is an mth-order polynomial in η_2 and an mth-order polynomial in $\tilde{\eta}_2$, assuming η_1 is fixed. As has been discussed in previous work [16], on decrease of coherence the original mth-order vortex will break into m first-order vortices, with m negative first-order vortices approaching from infinity. The mth-order vortex is robust under small decreases of coherence; however, in the limit of low

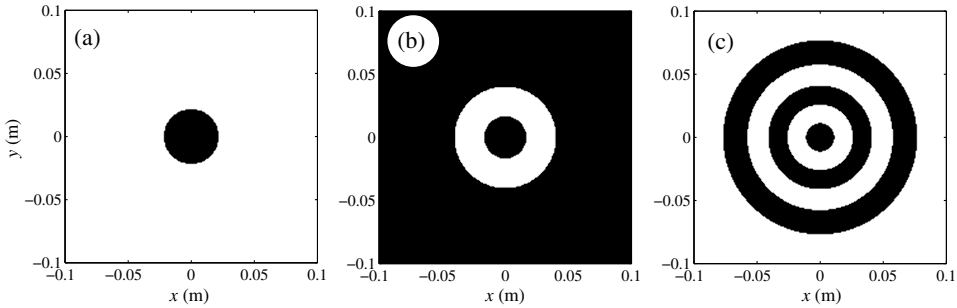

Fig. 3. Phase of $E(\mathbf{r})$, for (a) $m = 1$, (b) $m = 2$, and (c) $m = 5$. Here we have taken $\sigma = 1$ cm, $\alpha = 5 \times 10^{-6}\alpha_{\max}$, and $z = 2000$ m. Black indicates a phase of 0, white indicates a phase of π.

coherence, there will be a net topological charge of zero in the region near the origin.

It is difficult to directly measure these correlation vortices, which requires the phase of $\hat{W}$ to be measured with one point fixed, using for instance a Young's interference experiment. An alternative approach, first introduced by [22], is to measure the cross-correlation function of the field, i.e.,

$$E(\mathbf{r}) = \hat{W}(\mathbf{r}, -\mathbf{r}). \tag{32}$$

This approach is much easier to implement experimentally, and we use it here to study theoretically the correlation singularities of tvGSMs. With some effort, one can readily show that

$$E(\mathbf{r}) = \frac{1}{A^{2m+2}} \sum_{k=0}^{m} \binom{m}{k}^2 \Gamma(k+1) \left[-\frac{|J|^2 r^2}{A^2}\right]^{m-k}, \tag{33}$$

with

$$J \equiv \frac{A^2}{1 - i\gamma} - \frac{iz}{k_0 \Delta^4 |\beta|^2} - \frac{\pi\alpha}{|\beta|^2}. \tag{34}$$

This is an mth-order polynomial in r^2 with real coefficients, and due to the presence of the minus signs in the sum, we expect that we will in general get m zeros of this polynomial, or m dark rings in the cross-correlation function. This is illustrated for several vortex orders in Fig. 3. The rings, indicated by π phase jumps in the phase of the field, are roughly, but not exactly, spaced equally in radius.

The topological charge of the underlying vortex can be found simply by counting the number of dark rings or, equivalently, the number of phase jumps. A decrease in coherence results in an increase in the radii of the rings, though the size saturates for sufficiently large σ. It is to be noted conversely that, in the coherent limit, the radii of the rings shrink to zero.

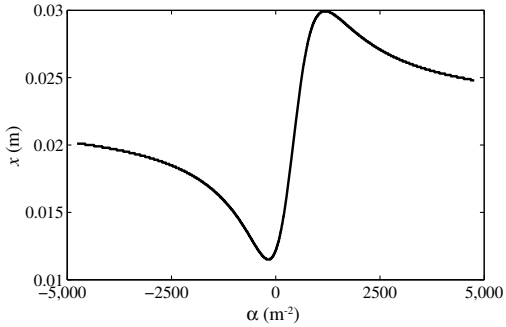

Fig. 4. Radius of the zero ring for a tvGSM of order $m = 1$, with $\sigma = 2$ cm, $z = 2$ km. The range of α is $-5 \times 10^{-5}\alpha_{\max} < \alpha < 5 \times 10^{-5}\alpha_{\max}$.

The dependence of the topology on the twist parameter is non-trivial, as illustrated in Fig. 4. The minimum radius is not at $\alpha = 0$, but at a slightly negative value. We interpret this as having to do with the counterbalance between the positive twist of the underlying vortex mode and the negative twist introduced by α. This will be of more significance in the next section.

5. ORBITAL ANGULAR MOMENTUM

We now consider the orbital angular momentum characteristics of tvGSMs. In general, the angular momentum of a beam of light is a combination of spin (polarization) and orbital (phase) angular momentum, and must be treated vectorially. If we assume that the field is unpolarized, then the z-component of the orbital angular momentum density $L_z(\mathbf{r}, z)$ can be expressed in terms of a single scalar cross-spectral density in the form (see [23] and Section 9.8 of [3])

$$L_z(\mathbf{r}, z) = \frac{\epsilon_0}{k_0} \mathrm{Im}\left\{\frac{\partial}{\partial \phi_2} W(\mathbf{r}_1, \mathbf{r}_2)\right\}_{\mathbf{r}_1 = \mathbf{r}_2 = \mathbf{r}}. \tag{35}$$

With some significant mathematical gymnastics, one can finally arrive at an expression of the form

$$L_z(\mathbf{r}, z) = \frac{\epsilon_0}{k} C(z) \exp[-r^2/\sigma_S^2] \times \left\{\frac{2\pi\alpha}{A^2|\beta|^2\Delta^2} \sum_{k=0}^{m} a_k |Q|^{2(m-k)} r^{2(m-k+1)} + R \sum_{k=0}^{m} a_k (m-k) |Q|^{2(m-k-1)} r^{2(m-k)}\right\}, \tag{36}$$

where $R = |G|^2 - |H|^2$.

We first look at the total orbital angular momentum of the beam in a cross section, which can be found by integrating $L_z(\mathbf{r}, z)$ over the transverse plane. We calculate the total average OAM per photon l_z, which is given by the expression

$$l_z = \hbar\omega \frac{\int L_z(\mathbf{r}, z) \mathrm{d}^2 r}{\int S_z(\mathbf{r}, z) \mathrm{d}^2 r}, \tag{37}$$

where $S_z(\mathbf{r}, \omega)$ is the z-component of the Poynting vector,

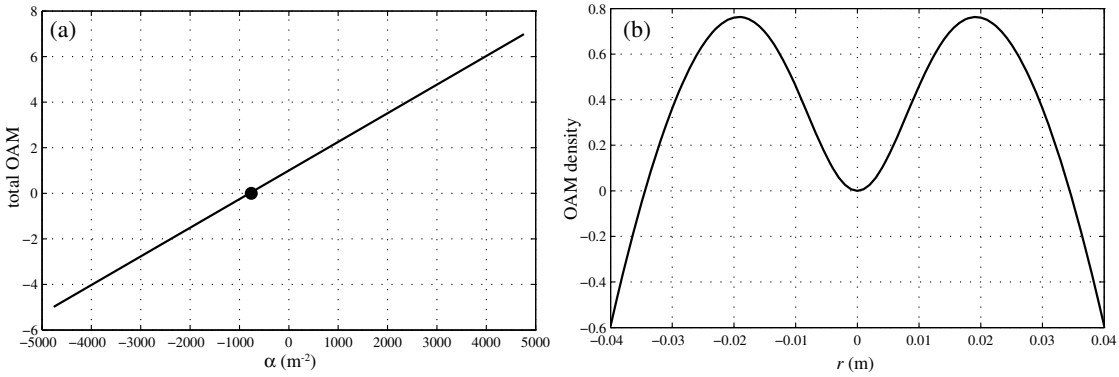

Fig. 5. Plots related to a zero net OAM beam. (a) The total OAM as a function of α, with $l_z = 0$ highlighted with a dot. (b) The OAM density m_z as a function of r, showing the positively rotating core and negatively rotating outskirts. Here $m = 1$, $\sigma = 1$ cm, and $\alpha = -809$ m^{-2}.

$$S_z(\mathbf{r},\omega) = \frac{k}{\mu_0\omega} C(z) \exp[-r^2/\sigma_S^2] \sum_{k=0}^{m} a_k |Q|^{2(m-k)} r^{2(m-k)}. \tag{38}$$

In the plane $z = 0$, the value of l_z can be calculated, with some effort, to be of the form

$$l_z = \hbar \left\{ m + 4\pi\alpha\sigma^2 \left[1 + \frac{m\frac{\Delta^2}{2\sigma^2}}{1+\frac{\Delta^2}{2\sigma^2}} \right] \right\}. \tag{39}$$

The OAM due to the vortex ends up being independent of the spatial coherence of the source; this can be attributed to the observation that the OAM is an intrinsic quantity of Laguerre–Gauss modes [24], and therefore independent of the choice of the beam axis $\mathbf{r}_0$. The second term of Eq. (39), which is the contribution of the twist, depends on the twist parameter, the relative beam wander Δ/σ, as well as the order m of the vortex.

The total OAM should be constant on propagation, and this can be confirmed readily by analytically evaluating the integrals of Eq. (37) and plotting the behavior of l_z as a function of distance.

Another significant OAM property of the beam is the local OAM density per photon m_z, which we may define as

$$m_z = \hbar\omega \frac{L_z(\mathbf{r},z)}{S_z(\mathbf{r},z)}. \tag{40}$$

It has been noted [17] that a tGSM beam acts like a pure rigid body rotator, with $m_z \sim r^2$, while a pure Rankine beam acts like a rigid body rotator near its core and a fluid body rotator, with $m_z \sim$ constant, in its outskirts. A tvGSM beam will act like a rigid body rotator in its core, as well; for small r, we may write the approximate form as

$$m_z \approx \hbar \left\{ \frac{2\pi\alpha}{A^2\Delta^2} r^2 + \frac{a_{m-1}}{a_m} R r^2 \right\}. \tag{41}$$

The combination of two distinct types of OAM in tvGSM beams allows for beams with behaviors not previously seen. The first possibility is to create a beam that has a zero total OAM, by using a positive m with a negative α. For a given set of parameters, we can readily find a value of α for which the total OAM is zero, as illustrated in Fig. 5(a). Looking at the OAM density in Fig. 5(b), we see that the beam has a positive OAM core surrounded by negative OAM in the outskirts. We therefore have a beam with counter-rotating regions.

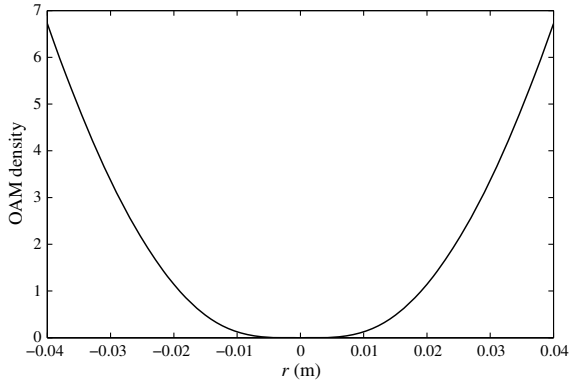

Fig. 6. OAM density for a beam with suppressed quadratic dependence, leaving a "dead zone" in its core. Here $m = 1$, $\sigma = 1$ cm, and $\alpha = 2.381 \times 10^3$ m^{-2}.

It is interesting to note that the beam of Fig. 5 has a non-zero average topological charge, yet a zero OAM. Conversely, it is readily seen that a twisted GSM beam (or a tvGSM with $m = 0$) has a zero topological charge, but non-zero OAM. It has long been recognized that there is not a simple relationship between OAM and topological charge [25], and these two cases represent extreme examples of the discrepancy that can arise.

A second unusual possibility is to create a beam that has a "dead zone" of circulation in its core, by suppressing the quadratic part of the OAM density. By the use of Eq. (41), we can find a value of α for which the quadratic component vanishes. The resulting OAM density is illustrated in Fig. 6, and it has a quartic dependence on radial distance r.

These behaviors demonstrate that it is not only possible to control the total OAM in partially coherent beams, but to control its transverse distribution in space.

6. CONCLUSIONS

A new class of partially coherent beams possessing OAM, called twisted vortex Gaussian Schell-model beams, has been intro-

duced and its properties described. Such beams not only have well-defined topological characteristics that are of potential use for FSOC, but have unprecedented control over their OAM characteristics, which may result in novel uses not only in FSOC but also in the development of light-driven micromachines, such as discussed, for example, in [8,26,27].

It is important to note that the "twist" OAM can only be produced using partially coherent beams. This research indicates that the use of partially coherent beams provides additional control over the OAM characteristics of light, and should be considered as an option in any OAM-based application.

APPENDIX A: PROPAGATION OF A TILTED VORTEX MODE

We may derive Eq. (8) from Eq. (7) by use of the Fresnel propagation formula,

$$U(\mathbf{r},z) = -\frac{ik_0}{2\pi z}\int U_0(\mathbf{r}')\exp\left[i\frac{k_0}{2z}|\mathbf{r}-\mathbf{r}'|^2\right]\mathrm{d}^2r', \tag{A1}$$

where $U_0(\mathbf{r})$ is the field in the source plane. First, for simplicity, Eq. (7) is centered on the origin by making the coordinate transformation $x \to x + x_0$, $y \to y + y_0$, which makes it reduce to

$$U_0(\mathbf{r}) = \frac{U_0}{\Delta^m}\exp[-(x^2+y^2)/2\Delta^2]\exp[2\pi i\alpha(x_0y - y_0x)][x+iy]^m. \tag{A2}$$

On expanding the Fresnel kernel, the integral may be written in the form

$$U(\mathbf{r},z) = S(x,y,z)\int \exp[-p(x'^2+y'^2)]\exp[i(q_xx' + q_yy')] \times [x'+iy']^m\mathrm{d}x'\mathrm{d}y', \tag{A3}$$

with

$$p \equiv \frac{1}{2\Delta^2} - \frac{ik_0}{2z}, \tag{A4}$$

$$q_x \equiv -2\pi\alpha y_0 - \frac{k_0}{z}x, \tag{A5}$$

$$q_y \equiv 2\pi\alpha x_0 - \frac{k_0}{z}y, \tag{A6}$$

and

$$S(x,y,z) \equiv -\frac{ik_0}{2\pi z}\frac{U_0}{\Delta^m}\exp[ik_0z]\exp\left[i\frac{k_0}{2z}(x^2+y^2)\right]. \tag{A7}$$

The integral is of a standard form, which can be evaluated in polar coordinates using Bessel functions, and the result may be written as

$$U(\mathbf{r},z) = 2\pi i^m S(x,y,z)\frac{(q_x+iq_y)^m}{(2p)^{m+1}}\exp\left[-\frac{q_x^2+q_y^2}{4p}\right]. \tag{A8}$$

The values of p, q_x, and q_y must be substituted back into this expression, and the opposite coordinate transformation made to undo the earlier one: $x \to x - x_0$, $y \to y - y_0$. The result of Eq. (8) then follows.

APPENDIX B: DERIVING THE TVGSM CROSS-SPECTRAL DENSITY

To derive Eq. (11), it is convenient to first express all transverse variables as complex numbers, namely, $\eta = x + iy$ and $\eta_0 = x_0 + iy_0$. With this, Eq. (8) may be written as

$$U(\mathbf{r},z) = \frac{U_0}{\beta}e^{ik_0z}\frac{[\eta-(1+i\gamma)\eta_0]^m}{(\Delta\beta)^m}\exp[-|\eta-\eta_0|^2/2\Delta^2\beta] \times \exp\left[-i\frac{2\pi^2\alpha^2z}{\beta k_0}|\eta_0|^2\right]\exp[\pi\alpha(\eta\tilde{\eta}_0 - \tilde{\eta}\eta_0)/\beta]. \tag{B1}$$

We use this expression twice in Eq. (3), giving us an expression for the cross-spectral density. We may group terms by their power of η_0 and $\tilde{\eta}_0$, resulting in the compressed formula

$$W(\mathbf{r}_1,\mathbf{r}_2,z) = P_0\frac{|U_0|^2}{|\beta|^2}\frac{1}{|\Delta\beta|^{2m}}\exp[-|\eta_1|^2/2\Delta^2\tilde{\beta}] \times \exp[-|\eta_2|^2/2\Delta^2\beta]\int\exp[-A^2|\eta_0|^2] \times \exp[A\tilde{B}\eta_0 + AB\tilde{\eta}_0][\tilde{\eta}_1-(1-i\gamma)\tilde{\eta}_0]^m \times [\eta_2-(1+i\gamma)\eta_0]^m\mathrm{d}^2r_0, \tag{B2}$$

where A^2 is given as in Eq. (14), and we use a slightly unconventional notation to define

$$AB = \frac{\eta_1}{2\Delta^2\tilde{\beta}} + \frac{\eta_2}{2\Delta^2\beta} - \frac{\pi\alpha\eta_1}{\tilde{\beta}} + \frac{\pi\alpha\eta_2}{\beta}, \tag{B3}$$

$$A\tilde{B} = \frac{\tilde{\eta}_1}{2\Delta^2\tilde{\beta}} + \frac{\tilde{\eta}_2}{2\Delta^2\beta} + \frac{\pi\alpha\tilde{\eta}_1}{\tilde{\beta}} - \frac{\pi\alpha\tilde{\eta}_2}{\beta}. \tag{B4}$$

It is to be noted that B and $\tilde{B}$ are not strict complex conjugates of each other, but we adopt such a notation for brevity; it does not affect the outcome of the calculation.

We may now complete the square in the exponent, and write

$$W(\mathbf{r}_1,\mathbf{r}_2,z) = P_0\frac{|U_0|^2}{|\beta|^2}\frac{1}{|\Delta\beta|^{2m}}\exp[-|\eta_1|^2/2\Delta^2\tilde{\beta}] \times \exp[-|\eta_2|^2/2\Delta^2\beta]\exp[B\tilde{B}] \times \int\exp[-(A\eta_0 - B)(A\tilde{\eta}_0 - \tilde{B})] \times [\tilde{\eta}_1-(1-i\gamma)\tilde{\eta}_0]^m[\eta_2-(1+i\gamma)\eta_0]^m\mathrm{d}^2r_0. \tag{B5}$$

Now, noting that η_0 and $\tilde{\eta}_0$ are independent complex variables just as x_0 and y_0 are independent real variables, we make the coordinate transformation:

$$\eta_0 \to \eta_0 + B/A, \qquad \tilde{\eta}_0 \to \tilde{\eta}_0 + \tilde{B}/A. \tag{B6}$$

We also now use our definitions for $F(\mathbf{r}_1,\mathbf{r}_2,z)$ and $C(z)$, which allows us to write

$$W(\mathbf{r}_1,\mathbf{r}_2,z) = \frac{1}{\pi(1+\gamma^2)^m}\frac{C(z)F(\mathbf{r}_1,\mathbf{r}_2,z)}{A^{4m}}\int\exp[-A^2|\eta_0|^2] \times [\tilde{\eta}_1-(1-i\gamma)(\tilde{\eta}_0+\tilde{B}/A)]^m \times [\eta_2-(1+i\gamma)(\eta_0+B/A)]^m\mathrm{d}^2r_0. \tag{B7}$$

We now introduce our definitions of D_1 and D_2, and pull out a common factor of $1/A^{4m}$ from the integral. We now have

$$W(\mathbf{r}_1,\mathbf{r}_2,z)=\frac{1}{\pi}C(z)F(\mathbf{r}_1,\mathbf{r}_2,z)\int \exp[-A^2|\eta_0|^2][D_1-A^2\tilde{\eta}_0]^m \times[D_2-A^2\eta_0]^m \mathrm{d}^2r_0. \tag{B8}$$

We next use the binomial theorem to expand each of the D-terms; for example,

$$[D_1-A^2\tilde{\eta}_0]^m=\sum_{l=0}^{m}\binom{m}{l}(D_1)^{m-l}(-A^2\tilde{\eta}_0)^l. \tag{B9}$$

On substituting this sum into the integral, and a similar sum over k for the D_2 term, we get an integral which includes a rotationally symmetric exponential $\exp[-A^2\rho_0^2]$ and a double sum with terms of the form $(\tilde{\eta}_0)^l(\eta_0)^k$. If we integrate in polar coordinates, only terms for which $l=k$ will be non-zero, reducing the double sum into a single sum. The integral over ϕ then gives 2π, and we have

$$W(\mathbf{r}_1,\mathbf{r}_2,z)=2C(z)F(\mathbf{r}_1,\mathbf{r}_2,z)\sum_{k=0}^{m}\binom{m}{k}^2\frac{(D_1D_2)^{m-k}}{A^{4m}} \times\int_0^\infty \exp[-A^2\rho_0^2](A^4\rho_0^2)^k\rho_0\mathrm{d}\rho_0. \tag{B10}$$

We finally note that, with a change of variable to $u=A\rho_0$, the integral is of a standard form,

$$\int_0^\infty \exp[-u^2]u^{2k+1}\mathrm{d}u=\frac{\Gamma(k+1)}{2}. \tag{B11}$$

On substitution, we arrive at Eq. (11).

It should be noted that deriving the final form of $F(\mathbf{r}_1,\mathbf{r}_2,z)$, as given by Eq. (17), is also non-trivial. One must group together all the exponents that appear outside of the integral in Eq. (B5). Of these, one finds a cross term that depends on $\mathbf{r}_1\cdot\mathbf{r}_2$; treating this as the middle of a square of the form $|\mathbf{r}_1-\mathbf{r}_2|^2$, one can complete it to derive the term involving P^2. The twist phase separates out easily, leaving terms dependent only on r_1^2 and r_2^2 that can be grouped to get the final result.

Funding. Air Force Office of Scientific Research (AFOSR) (FA9550-16-1-0240).

REFERENCES

1. M. S. Soskin and M. V. Vasnetsov, "Singular optics," in *Progress in Optics*, E. Wolf, ed. (Elsevier, 2001), Vol. **42**, pp. 219–276.
2. M. R. Dennis, K. O'Holleran, and M. J. Padgett, "Singular optics: Optical vortices and polarization singularities," in *Progress in Optics*, E. Wolf, ed. (Elsevier, 2009), Vol. **53**, pp. 293–363.
3. G. J. Gbur, *Singular Optics* (CRC Press, 2017).
4. J. H. Lee, G. Foo, E. G. Johnson, and G. A. Swartzlander, Jr., "Experimental verification of an optical vortex coronagraph," Phys. Rev. Lett. **97**, 053901 (2006).
5. D. Palacios, D. Rozas, and G. A. Swartzlander, Jr., "Observed scattering into a dark optical vortex core," Phys. Rev. Lett. **88**, 103902 (2002).
6. A. Jesacher, S. Fürhapter, S. Bernet, and M. Ritsch-Marte, "Shadow effects in spiral phase contrast microscopy," Phys. Rev. Lett. **94**, 233902 (2005).
7. N. B. Simpson, K. Dholakia, L. Allen, and M. J. Padgett, "Mechanical equivalence of spin and orbital angular momentum of light: an optical spanner," Opt. Lett. **22**, 52–54 (1997).
8. K. Ladavac and D. G. Grier, "Microoptomechanical pumps assembled and driven by holographic optical vortex arrays," Opt. Express **12**, 1144–1149 (2004).
9. G. Gibson, J. Courtial, M. J. Padgett, M. Vasnetsov, V. Pas'ko, S. M. Barnett, and S. Franke-Arnold, "Free-space information transfer using light beams carrying orbital angular momentum," Opt. Express **12**, 5448–5456 (2004).
10. J. Wang, J.-Y. Yang, I. M. Fazal, N. Ahmed, Y. Yan, H. Huang, Y. Ren, Y. Yue, S. Dolinar, M. Tur, and A. E. Willner, "Terabit free-space data transmission employing orbital angular momentum multiplexing," Nat. Photonics **6**, 488–496 (2012).
11. G. Gbur and R. K. Tyson, "Vortex beam propagation through atmospheric turbulence and topological charge conservation," J. Opt. Soc. Am. A **25**, 225–230 (2008).
12. J. A. Anguita, M. A. Neifeld, and B. V. Vasic, "Turbulence-induced channel crosstalk in an orbital angular momentum-multiplexed free-space optical link," Appl. Opt. **47**, 2414–2429 (2008).
13. B. Rodenburg, M. P. J. Lavery, M. Malik, M. N. O'sullivan, M. Mirhosseini, D. J. Robertson, M. Padgett, and R. W. Boyd, "Influence of atmospheric turbulence on states of light carrying orbital angular momentum," Opt. Lett. **37**, 3735–3737 (2012).
14. G. Gbur, "Partially coherent beam propagation in atmospheric turbulence [invited]," J. Opt. Soc. Am. A **31**, 2038–2045 (2014).
15. R. Simon and N. Mukunda, "Twisted Gaussian Schell-model beams," J. Opt. Soc. Am. A **10**, 95–109 (1993).
16. C. S. D. Stahl and G. Gbur, "Partially coherent vortex beams of arbitrary order," J. Opt. Soc. Am. A **34**, 1793–1799 (2017).
17. G. Gbur, "Partially coherent vortex beams," Proc. SPIE **10549**, 1054903 (2018).
18. D. Ambrosini, V. Bagini, F. Gori, and M. Santarsiero, "Twisted Gaussian Schell-model beams: a superposition model," J. Mod. Opt. **41**, 1391–1399 (1994).
19. E. Wolf, "New theory of partial coherence in the space-frequency domain. part 1: spectra and cross-spectra of steady-state sources," J. Opt. Soc. Am. **72**, 343–351 (1982).
20. G. Gbur, T. D. Visser, and E. Wolf, "'Hidden' singularities in partially coherent fields," J. Opt. A **6**, S239–S242 (2004).
21. F. Gori and M. Santarsiero, "Devising genuine spatial correlation functions," Opt. Lett. **32**, 3531–3533 (2007).
22. D. M. Palacios, I. D. Maleev, A. S. Marathay, and G. A. Swartzlander, Jr., "Spatial correlation singularity of a vortex field," Phys. Rev. Lett. **92**, 143905 (2004).
23. S. M. Kim and G. Gbur, "Angular momentum conservation in partially coherent wave fields," Phys. Rev. A **86**, 043814 (2012).
24. A. T. O'Neil, I. MacVicar, L. Allen, and M. J. Padgett, "Intrinsic and extrinsic nature of the orbital angular momentum of a light beam," Phys. Rev. Lett. **88**, 053601 (2002).
25. M. Berry, "Paraxial beams of spinning light," Proc. SPIE **3487**, 6–11 (1998).
26. P. Galajdá and P. Ormos, "Complex micromachines produced and driven by light," Appl. Phys. Lett. **78**, 249–251 (2001).
27. M. E. J. Friese, H. Rubinsztein-Dunlop, J. Gold, P. Hagberg, and D. Hanstorp, "Optically driven micromachine elements," Appl. Phys. Lett. **78**, 547–549 (2001).